RSC Advances

This is an *Accepted Manuscript*, which has been through the Royal Society of Chemistry peer review process and has been accepted for publication.

Accepted Manuscripts are published online shortly after acceptance, before technical editing, formatting and proof reading. Using this free service, authors can make their results available to the community, in citable form, before we publish the edited article. This *Accepted Manuscript* will be replaced by the edited, formatted and paginated article as soon as this is available.

You can find more information about *Accepted Manuscripts* in the Information for Authors.

Please note that technical editing may introduce minor changes to the text and/or graphics, which may alter content. The journal's standard Terms & Conditions and the Ethical guidelines still apply. In no event shall the Royal Society of Chemistry be held responsible for any errors or omissions in this *Accepted Manuscript* or any consequences arising from the use of any information it contains.

ROYAL SOCIETY OF CHEMISTRY

www.rsc.org/advances

Please do not adjust margins

RSC Advance

ARTICLE

Rapid Adsorption Removal of Arsenate by Hydrous Cerium Oxide-Graphene Composite

Received 00th January 2015,
Accepted 00th January 2015

DOI: 10.1039/x0xx00000x

www.rsc.org/

Ling Yu [a], Ying Ma [b], Choon Nam Ong [a], Jianping Xie [b], Yanbiao Liu [a,*]

The arsenic contamination has posed a health risk to millions of people around the world. In this study, a novel adsorbent, hydrous cerium oxide modified graphene (GNP-HCO), was synthesized for arsenic removal from aqueous solution. In the kinetics study, >88% of equilibrium adsorption capacity of arsenate (As(V)) can be achieved within the initial 20 min. Such rapid adsorption rate showed its promising potential towards actual application. The experimental data was better described by the Langmuir isotherm model, and the maximum adsorption capacities were 62.33 and 41.31 mg-As/g at pH 4.0 and 7.0, respectively, which are much higher than many modified carbon-based adsorbents previously reported. Phosphate appeared to be the most severe competitive interference on arsenic adsorption. Furthermore, the adsorption removal of arsenic adsorbent from surface water matrix was also evaluated and the results demonstrated that only 15 mg/L adsorbent was required to reduce the arsenic concentration from 100 μg/L to <10 μg/L. X-ray photoelectron spectroscopy (XPS) analysis indicated that the major chemical state of cerium (Ce) element in the adsorbent was +IV and hydroxyl group might be involved in the adsorption process.

Introduction

Arsenic-contamination in natural surface water and ground water can lead to severe human health effects. It is estimated that over 137 million people in more than 70 countries are facing the risk of arsenic contamination of drinking water.[1] It has been reported that several types of cancers may be caused by long-term exposure to arsenic.[2] On the basis of arsenic's toxicity, the World Health Organization (WHO) and U.S. Environmental Protection Agency (USEPA) have set a maximum contaminant level (MCL) of arsenic in drinking water as 10 μg/L. Various treatment technologies, including chemical precipitation,[3] ion exchange,[4] biological processes,[5] physical adsorption,[6] and membrane processes,[7] have been applied to remove arsenic from aqueous solution. Among them, adsorption process was considered to be one of the most promising technologies due to ease in operation, cost-effectiveness and environmental friendliness.

Till now, a wide range of adsorbents such as zero-valent iron,[8, 9] activated carbon or its modified materials,[10] metal oxides (e.g. Fe_3O_4,[11] MnO_2,[12] CeO_2,[13] TiO_2,[14] and ZrO_2[15]) as well as industrial/agriculture wastes[16] have been extensively explored towards arsenic removal. Of these adsorbents, metal oxides especially rare earth metal oxides have attracted much attention due to their excellent adsorption performance in removing anionic contaminants (e.g. arsenic). An ideal arsenic adsorbent should possess several advantages such as rapid adsorption kinetics, high adsorption capacity, excellent stability and strong affinity towards arsenic. Nevertheless, despite significant progress in the arsenic adsorption achieved to date, there are still some practical limitations to be addressed.

To overcome these limitations, researchers have been trying to develop composite adsorbents to combine the advantages of both.[17] For example, metal oxides have been impregnated onto the surface of other porous carbon materials, such as activated carbon, for adsorbing removal of various organic compounds from water.[18-20] It hence can be envisaged that composite adsorbent could combine the advantages of the carbon materials with high specific surface and suitable metal oxides with high affinity to arsenic.

Graphene, a 2D one-atom-thick layer of graphite, has attracted much attention recently due to its amazing properties.[21, 22] It has been widely used in organic pollutants removal,[23, 24] energy storage devices,[25] flexible transparent electrodes,[26] solar cells,[27] and electronics and optoelectronics.[28] However, less attention has been paid to the adsorption removal of inorganic pollutants such as arsenic by graphene or graphene-based composites. In this study, a novel and high-performance hydrous cerium oxide (HCO) modified graphene nanoplatelets (GNP) composite was developed to address the key limitations of slow adsorption kinetics for arsenic removal. Over here, a facile wet-chemistry route was used to coat HCO onto the GNP surface. Various advanced characterization techniques (e.g. FESEM, EDS, and XPS) were adopted to study the morphological and compositional information of the as-synthesized adsorbents. Adsorption kinetics and isotherm

[a] NUS Environmental Research Institute, National University of Singapore, 5A Engineering Drive 1, #02-01, 117411, Singapore. Fax: +65 6872 1320; Tel: +65 6516 7386; E-mail: eriliuyb@nus.edu.sg.
[b] Department of Chemical and Biomolecular Engineering, National University of Singapore, 117585, Singapore.
† Electronic Supplementary Information (ESI) available. See DOI: 10.1039/x0xx00000x

RSC Advances Accepted Manuscript

Please do not adjust margins

studies were comparatively conducted and the effect of solution pH, natural organic matter (NOM) and competitive anions on the adsorption performance were systematically studied. The adsorption removal of arsenic in surface water samples was carried out as well to further validate the effectiveness of the adsorbents, and the possible mechanisms involved were discussed.

Material and methods

Materials

The chemicals including $Ce(NO_3)_3 \cdot 6H_2O$, $Na_2HAsO_4 \cdot 7H_2O$, Na_2SO_4, $NaHCO_3$, NaF, KH_2PO_4, NaOH, HNO_3 and ethanol were of analytical grade and purchased from Sigma-Aldrich (St. Louis, MO) without further purification. Humic acid (HA) used to represent typical natural organic matter (NOM) in this study was purchased from Sigma-Aldrich (Product Number: H16752). C-grade Graphene nanoplatelets (GNP) were purchased from XG Sciences (Lansing, MI). The stock solution of arsenate was prepared by dissolving a certain amount of $Na_2HAsO_4 \cdot 7H_2O$ into deionized (DI) water and the working solutions were obtained by freshly diluting the arsenic stock solution with DI water.

Preparation of GNP-HCO Composite

A certain amount of GNP was dispersed at a concentration of 0.5 mg/mL into ethanol by ultrasonication for at least 30 min. $Ce(NO_3)_3$ was then added into the solution to bring a concentration of cerium to 0.01 M and stirred at 700 rpm overnight. Thereafter, 0.5 M NaOH/ethanol solution was added dropwise into the solution under continuous stirring until pH = 10 ± 0.1. Finally, the formed particles were collected, washed sequentially by DI water and ethanol for several times, and then dried in the oven for 12 h at 70 ºC. As a comparison, the HCO was synthesized via a similar route without the addition of GNP.

Characterizations of Adsorbent

Morphology and elemental analysis

The surface morphology of adsorbent was studied using a field emission scanning electron microscope (FESEM) (JSM6700F, JEQ, Japan) equipped with an energy dispersive X-ray spectroscopy (EDX, JEOL JED 2300). The samples were first coated with a thin film of platinum on the surface for electrical conductive purpose. The morphology of the adsorbents was further analyzed by the transmission electron microscopy (TEM) (JEOL JEM-2100).

Determination of point of zero charge

The point of zero charge (pH_{PZC}) was estimated by the pH drift method.[29] The adsorbent was first suspended in 0.01 M $NaNO_3$ for 24 h, after which the pH change became insignificant. 50-mL suspension was then adjusted to a series of pH values using either NaOH or HNO_3 solution. After agitation for 60 min to achieve equilibrium, the initial pH was measured; then 1.5-g $NaNO_3$ was added to each suspension solution to bring final electrolyte concentration to approximately 0.45 M. After another 3 h, the final pH was measured. The results, plotted as ΔpH (final pH- initial pH) against final pH, yielded the pH_{PZC} as the pH at which ΔpH equals to 0.

Adsorption Experiment

Adsorption kinetics

The adsorption kinetics experiment was carried out at initial arsenic concentration ($[As]_0$) of 10 mg/L and the adsorbent dosage (m) of 0.1 g/L. The solution pH value was controlled at 4.0 during the adsorption process. The samples were taken at different time intervals and the experiments were completed in at least duplicate. The mean values were present and used for modelling study. After filtering with 0.45 μm cellulose membrane (Whatman, Sigma-Aldrich), the arsenic concentration was measured by an inductively coupled plasma optical emission spectrometer (ICP-OES, Perkin-Elmer Optima 3000).

Influence of pH and competitive factors

The experiment on pH effect was conducted with an initial arsenic concentration of 10 mg/L, and solution pH values were adjusted from 3 to 10 by adding a certain amount of HNO_3 and/or NaOH. The adsorption experiment was conducted at room temperature (T = 25 ± 1°C) for 12 h. Other procedures were the same as that of kinetics experiment.

The presence of competitive factors such as HA, NaF, Na_2SO_4, $NaHCO_3$ or KH_2PO_4 in the water may affect the adsorption performance as well. These substances were respectively added into the arsenic solution to study their influence on the arsenic uptake. The procedures were the same as that used in the pH effect study, except that the pH was fixed at 4.0.

Adsorption isotherm

Experiments for studying arsenic adsorption isotherm were conducted at room temperature and pH 4.0 and 7.0 by following the kinetics procedures. 0.01-g adsorbent was added to 100-mL arsenic solution with concentrations ranging from 1 to 80 mg/L.

Performance in surface water

To evaluate the arsenic removal performance in surface water, the Singapore reservoir water was employed (the water characteristics can be found in Table S1) to study the removal efficiency of arsenic under different adsorbent dosages. In the experiment, Na_2HAsO_4 was spiked into the water sample so that the concentration of 100 μg-As/L can be obtained, which represents a typical situation of arsenic contaminated surface water. After adsorption with various amounts of adsorbent, the removal efficiency of arsenic was measured with ICP-OES.

XPS Analysis

RSC Advances Accepted Manuscript

 This journal is © The Royal Society of Chemistry 2015

The surface of adsorbents before and after arsenic adsorption was analyzed by an X-ray photoelectron spectroscopy (XPS) (Kratos AXIS Ultra^{DLD}, Kratos Analytical Ltd). The XPS results were collected in binding energy forms and fitted using a non-linear least-square curve fitting program (XPSPEAK41 Software). To compensate for the charging effect, all spectra were calibrated with graphitic carbon as reference at a binding energy of 284.8 eV. For the elements of cerium and oxygen, the spectra were deconvolved with the subtraction of a linear background and a Gaussian (20%)-Lorentzian (80%) mixed function.

Results and discussion

Characterizations of adsorbent

The surface morphology and element distribution of the as-synthesized GNP-HCO adsorbent were characterized by FESEM (inset) and EDS analysis, as displayed in Fig. 1a. The aggregation of the GNP-HCO particles was observed because the heat drying was applied into the synthesis process of adsorbents. It is evident that a dense particle layer was formed on the surface of GNP, which consisted nano-sized spherical particles (Fig. S1). On the basis of the EDS spectrum, cerium (Ce) element can be detected from the GNP-HCO adsorbent, which indicates that HCO has been successfully coated on the surface of GNP.

The value of point of zero charge (pH_{PZC}) of the adsorbent is determined to be approximately 6.0 (Fig. 1b). The surface charge of the adsorbent highly depends on the solution pH.

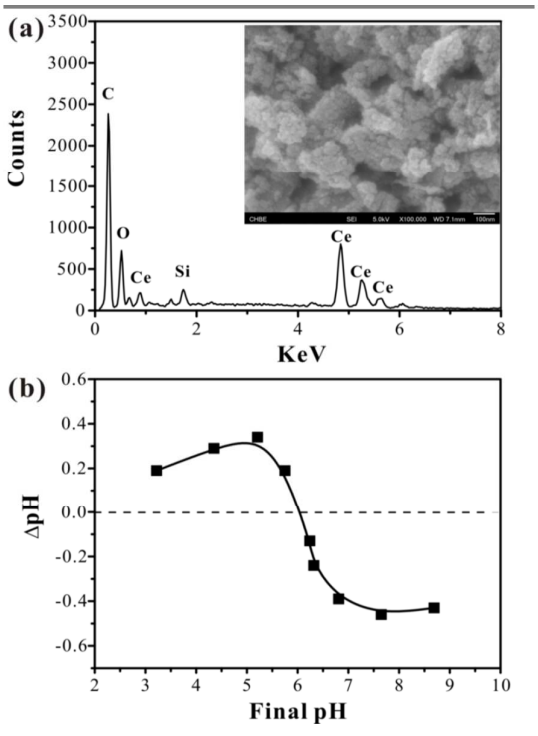

Fig. 1 Characterization of the GNP-HCO adsorbent: (a) FESEM (inset) and EDS analysis; (b) point of zero charge.

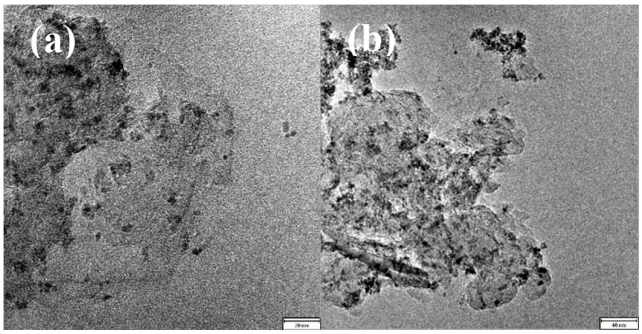

Fig. 2 TEM images of the GNP-HCO adsorbent before (a) and after (b) As-loaded.

When the solution pH is above its pH_{PZC}, negative charges can be readily formed on the surface of the adsorbent, which is unfavorable for the uptake of anion because of the enhanced electrostatic repulsion between the adsorbent surface and the target anions. In contrast, the adsorbent would be positively charged at pH < pH_{PZC}, which is favorable for the efficient arsenic uptake.

TEM analysis was further conducted to examine the change of the morphology of the GNP-HCO adsorbent before and after arsenic loading, as shown in Fig. 2. It is clearly seen that the highly transparent carbon sheet is decorated randomly by the deep-coloured particles with the size of ~10 nm, indicating that the nano-sized HCO particles have been uniformly loaded on the surface of the GNP. After the adsorption, there is no obvious change in the structure of the GNP-HCO adsorbent. The highly dispersed nanoparticles on the thin GNP layer would be beneficial for the adsorption process compared to the pure HCO particle. As well known, the aggregation phenomenon widely occurs in the preparation of metal oxide nanoparticles due to their high surface energy.

Adsorption kinetics

An extremely rapid adsorption behavior of arsenate onto the GNP-HCO adsorbent can be observed in Fig. 3. About 88.3% of equilibrium adsorption capacity of GNP-HCO can even be achieved within the first 20 min, with an initial arsenate

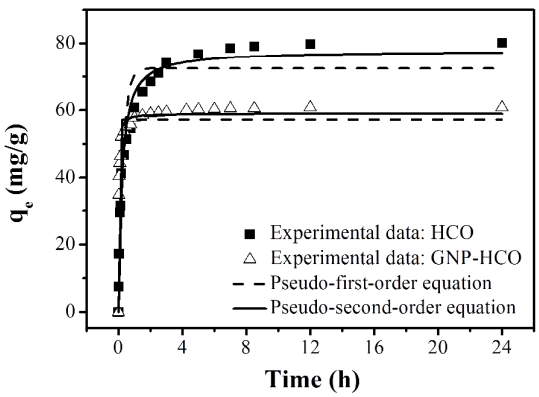

Fig. 3 Adsorption kinetics of arsenate. $[As(V)]_0$ = 10 mg/L, m = 0.1 g/L, and pH = 4.0.

RSC Advances Accepted Manuscript

Table 1 Parameters of pseudo-first and -second order equations ([As]$_0$ = 10 mg/L).

Adsorbent	Pseudo-first-order			Pseudo-second-order		
	q_e (mg/g)	k_1 (h^{-1})	r^2	q_e (mg/g)	k_2 ($g \cdot mg^{-1} \cdot h^{-1}$)	r^2
GNP-HCO	57.17	40.87	0.89	58.96	1.019	0.97
HCO	72.38	3.60	0.92	77.75	0.066	0.98

concentration of 10 mg/L. This finding is attractive for actual application because rapid adsorption rate at solid-solution interface may significantly reduce the required retention time in adsorption module and the cost of construction and operation.

It is also worthwhile to note that adsorption rate of GNP-HCO is much higher than that of HCO and other reported adsorbents, according to the rate constant (k_1 or k_2) obtained from the models.[30-32] The equilibrium adsorption of arsenate on GNP-HCO can be achieved within 2 h, while it takes more than 8 h for HCO alone. This may be due to the planar sheet structure and high surface area of GNP favors the diffusion of arsenate towards the active sites of HCO.

To better understand the adsorption mechanism, two empirical adsorption reaction models of pseudo-first-order model and pseudo-second-order model were applied to simulate the adsorption process.[33] The pseudo-first-order model is generally expressed as:

$$\ln(q_e - q_t) = \ln q_e - k_1 t \quad (1)$$

The pseudo-second-order model is based on the assumption that the rate of occupation of adsorption sites is proportional to the square of the number of unoccupied sites and can be described as:

$$\frac{t}{q_t} = \frac{1}{k_2 q_e^2} + \frac{t}{q_e} \quad (2)$$

where q_e and q_t are the amount of arsenate adsorbed by adsorbent at equilibrium and time t (mg/g), k_1 (h^{-1}) and k_2 ($g \cdot mg^{-1} \cdot h^{-1}$) is, respectively, the equilibrium constant of the pseudo-first and pseudo-second models, and t is the adsorption time (h).

The fitting parameters obtained from the kinetic models were summarized in Table 1. The experimental data can be better described by the pseudo-second-order model with a higher value of correlation coefficient (r^2 = 0.97). This indicates the adsorption process could be due to chemisorption.

Adsorption equilibrium

pH effect

The effect of solution pH on the removal of arsenate was experimentally examined in the pH range of 3.0-10.0. As shown in Fig. 4a, the uptake of arsenate on the GNP-HCO is slightly enhanced when solution pH increases from 3.0 to 4.0, and the maximum adsorption capacity of 61.03 mg-As/g is obtained at pH 4.0. The adsorption of arsenate onto the GNP-HCO drops when the solution pH increases further. Note that the adsorption capacity of 45.42 mg-As/g is still obtained at neutral condition. In contrast, nearly negligible adsorption of arsenate (around 1 mg-As/g) was observed for the pristine GNP. As expressed in Section Introduction, the GNP is more effective to remove organic pollutants from water and the loaded HCO nano-sized particles should be responsible for the highly efficient uptake of arsenate.

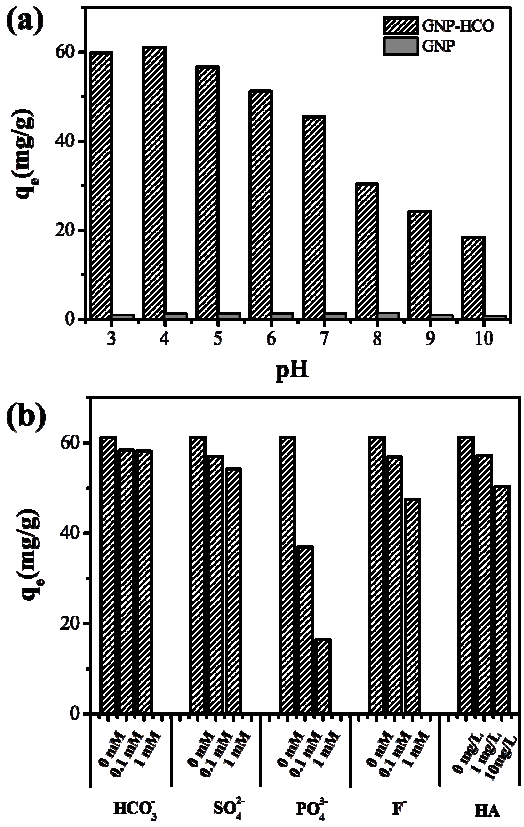

Fig. 4 Effect of solution pH (a) and co-existing anions and humic acid (b) on the arsenate adsorption: [As(V)]$_0$ = 10 mg/L, m = 0.1g/L, pH = 4.0 for (b), t = 12 h, T= 25 ± 1°C.

Based on the modeling result from MINEQL, $H_2AsO_4^-$ and $HAsO_4^{2-}$ are the dominant arsenate species in pH ranging from 3 to 10. The electrostatic interaction between the active sites on the adsorbent and arsenate may play an important role in the adsorption process. Since the pH_{PZC} of the adsorbent is determined to be ~6.0 (shown in Fig. 1b), stronger protonation of the functional groups on the surface of adsorbent can be achieved at pH <6.0, leading to enhanced electrostatic attraction between the positively charged active sites of the adsorbent and the negatively charged arsenate. However, the surface of the adsorbent becomes negative at pH >6.0 and, hence, the electrostatic repulsion effect would significantly hinder the uptake of arsenate. Furthermore, more OH- species are likely to present in the solution with the increase in solution pH and thus compete with arsenic towards the active sites of adsorbent.

Effect of competitive factors

RSC Advances Accepted Manuscript

This journal is © The Royal Society of Chemistry 2015

Since competitive anions such as bicarbonate, sulfate, phosphate fluoride, and natural organic matter (NOM) generally co-exist in natural water and groundwater, it is important to investigate the effect of their presence on arsenate adsorption. In this study, humic acid (HA) was chosen as a representative of NOM due to the prevalence of humic-like substances in surface waters and wastewater effluent. As shown in Fig. 4b, the presence of these competitive anions and HA has shown certain interferences on the arsenate adsorption. For example, the q_e at the presence of 1 mg/L and 10 mg/L HA was decreased by 7-18% in comparison with that obtained at their absence. Especially, a seriously negative effect on the adsorption of arsenate was observed in the presence of phosphate in solution. Similar adsorption behaviors of phosphate and arsenate may be due to the fact that both arsenate and phosphoric are in the form of triprotic acid, and with similar ionization constants.[32] Many previous studies have reported that the strong competition between arsenate ions and phosphate during the adsorption process.[34-37] However, it is noted that in the present study, when the concentration of phosphate in solution reaches 1 mM, nearly ten times of arsenate concentration (0.13 mM), an adsorption capacity of 16.47 mg-As/g can still be obtained.

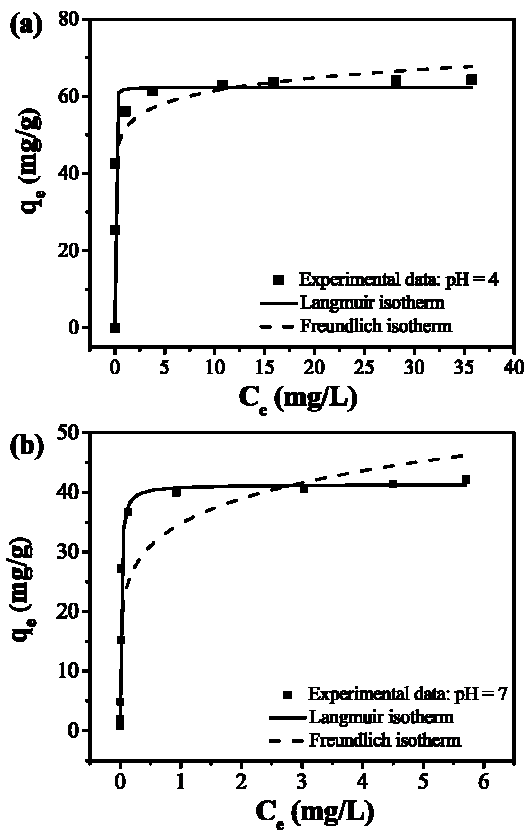

Fig. 5 Adsorption isotherms of arsenate on the adsorbent: (a) pH =4.0; (b) pH =7.0. m = 0.1 g/L, t = 12 h, T= 25 ± 1°C.

Table 2 Langmuir and Freundlich isotherms for arsenate adsorption.

pH	Langmuir isotherm			Freundlich isotherm		
	q_{max} (mg/g)	B (L/mg)	r^2	K_f (L/g)	n	r^2
4.0	62.33	110.80	0.978	51.44	13.00	0.941
7.0	41.31	78.20	0.970	34.76	6.106	0.795

Adsorption isotherm

The adsorption isotherm was conducted at pH 4.0 and 7.0, and the modelling results from both Langmuir and Freundlich are shown in Fig. 5, and the related parameters are summarized in Table 2. Langmuir equation seems to work better in the description of experimental data. This further indicates that arsenate uptake is mainly controlled by a monolayer adsorption process.[38, 39] The maximum adsorption capacity of arsenate calculated by the Langmuir model is 62.33 and 41.31 mg-As/g under pH 4.0 and 7.0, respectively. As a control adsorbent, there is no obvious adsorption of arsenic observed on virgin GNP (<0.5 mg-As/g). Thus, the promising adsorption capacity of GNP-HCO adsorbent could be mainly attributed to the loading of the HCO. It is worthwhile to note that the effluent concentration of arsenate would meet the guideline of arsenic in drinking water (i.e. 10 μg/L) with an initial arsenate concentration of below 2 mg/L and neutral pH conditions. The excellent performance on the removal of arsenate further indicates its promising potential for the treatment of arsenic-contaminated drinking water. After the adsorption completed, the spent adsorbent was tried to be regenerated by soaking into strong base solution (0.1 M NaOH) for 1 h. However, the adsorption capacity of reused adsorbent was found much less than that of fresh adsorbent, e.g. the q_e has decreased by 72% (first time) and 84% (second time) after regenerated and reused, as displayed in Fig. S3. The reason for this could be mainly due to the strong affinity of arsenate towards the adsorbent that cannot be easily desorbed and hence the available adsorption sites cannot be fully recovered. This assumption was also supported by the pH effect study. As shown in Fig. 4a, the adsorption capacities of 24.19 and 18.37 mg-As/g can be still achieved at pH 9 and pH 10, which could further confirm the formation of the strong bond between arsenic and the adsorbent. On the other hand, the strong combination of arsenic with the adsorbent could avoid the secondary release of arsenic to water body and good for the practical applications. Also, the agglomeration among the GNP scaffolds caused by the strong π-π interaction may inevitably sacrifice some active adsorption sites. Hence, more efforts should be devoted to develop other more effective approaches to recover the adsorption ability of the promising adsorbent. Moreover, a comparison of the q_{max} for arsenic between the as-synthesized GNP-HCO adsorbent and some previously reported carbon based adsorbents are summarized in Table 3. The results demonstrate that the GNP-HCO adsorbent shows much better performance than most previously reported adsorbents, including some modified graphene materials.

RSC Advances Accepted Manuscript

Table 3 Comparison of maximum adsorption capacities for different adsorbents.

Adsorbent	Initial As conc. (mg/L)	Adsorbent dosage (g/L)	Max. As(V) adsorption capacity (mg/g)	Ref.
Iron hydroxide modified AC	0-1.5	0.75	1.25	[40]
Manganese-modified ACF	1.4-80	0.80	23.77	[41]
Fe_3O_4-MWNTs based electrodes	200-400	0.08	53	[42]
Fe_3O_4-graphene-MnO_2 composites	0.01-10	0.50	12.22	[30]
Cu_2O-reduced graphene oxide	0.25-2	0.09	4.807	[43]
Magnetite-reduced graphitic oxide	3-7	0.2	5.83	[31]
Magnetic graphene oxide	10-60	0.4	59.6	[44]
TiO_2-coated CNT filter	0.1-10	0.31	14.1	[45]
Zirconium dioxide impregnated GAC	0-0.12	0.03	8.95	[46]
Zero-valent iron modified AC	2	0.5-6	12.02	[47]
GNP-HCO	1-80	0.1	62.33	This study

Performance in surface water

To further explore the potential of the adsorbent in the treatment of arsenic-contaminated surface water, reservoir water was employed to study the arsenate removal under different adsorbent dosages. In the experiment, certain Na_2HAsO_4 was spiked into the water samples so that a concentration of 100 µg-As/L can be obtained, which represents a typical concentration of natural water in the risk of arsenic around the world.

As shown in Fig. 6, the arsenate can be effectively removed from reservoir water with relatively low adsorbent dosage, and the removal efficiency increases with the adsorbent dosage. for example, at an adsorbent dosage of 15 mg/L, the arsenate concentration in effluent can be lower than 10 µg/L, which meets the maximum contaminant level for arsenic in drinking water, and with a corresponding adsorption capacity of 6.4 mg-As/g. Therefore, the GNP-HCO adsorbent exhibits very high application potential in the arsenate removal from surface water.

XPS analysis

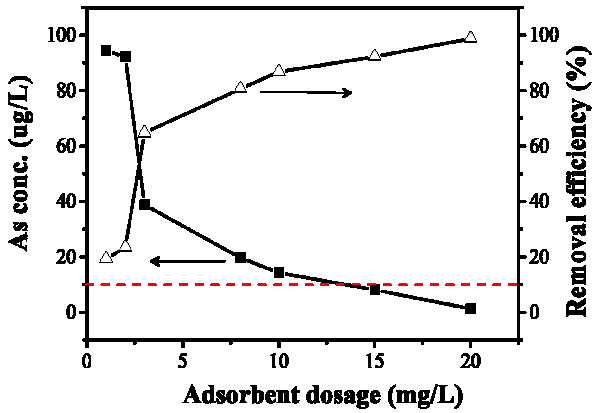

Fig. 6 Arsenate concentrations and removal efficiency of reservoir water sample as a function of adsorbent dosages. $[As]_0$ = 100 µg/L, pH = 6.78.

The adsorption mechanism of arsenate on the GNP-HCO adsorbent was further studied by the XPS analysis. The XPS wide scan spectra of both virgin and As-loaded adsorbent are shown in Fig. S2. The appearance of characteristic peaks of arsenic includes As 3d, As 3s and As LMM after the adsorption, indicating that arsenate has been successfully adsorbed. Furthermore, the peaks of Ce 4d, Ce MN and Ce 3d are also detected on the surface of both virgin and As-loaded adsorbent.

As shown in Fig. 7, the high-resolution XPS spectra of Ce 3d before and after arsenate adsorption mainly consist of the spin-orbit splitting of Ce $3d_{5/2}$ and Ce $3d_{3/2}$. Each separated peak is further divided into three component peaks due to a redistribution of the entire energy spectrum. The complex XPS spectra of Ce 3*d* were fitted by software to determine the chemical state of cerium element on the adsorbent according to the method described by Preisler et al.[48] Six fitting peaks labeled as blue color are determined as characteristic of Ce(IV), while other two peaks with red color are assigned to the

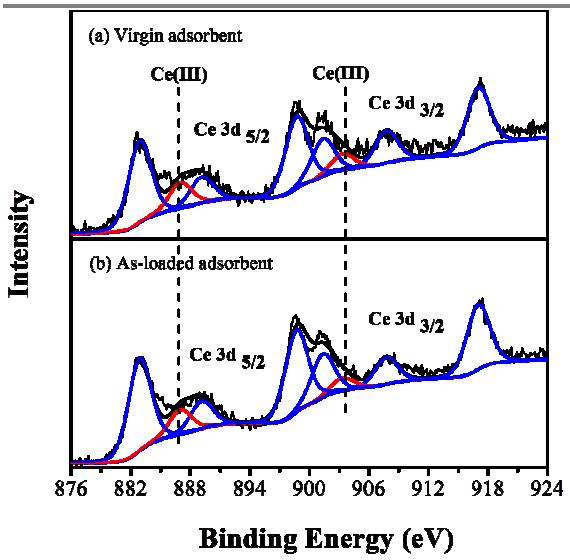

Fig. 7 XPS spectra of Ce 3d of the adsorbents: (a) virgin adsorbent; (b) As-loaded adsorbent.

RSC Advances Accepted Manuscript

This journal is © The Royal Society of Chemistry 2015

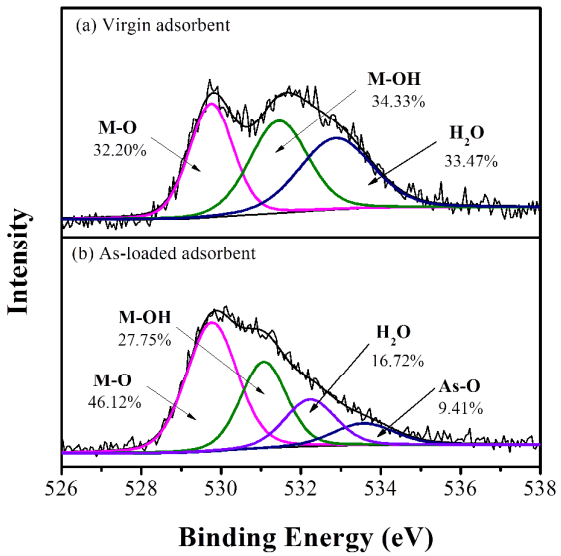

Fig. 8 XPS spectra of O 1s of the adsorbents: (a) virgin adsorbent; (b) As-loaded adsorbent.

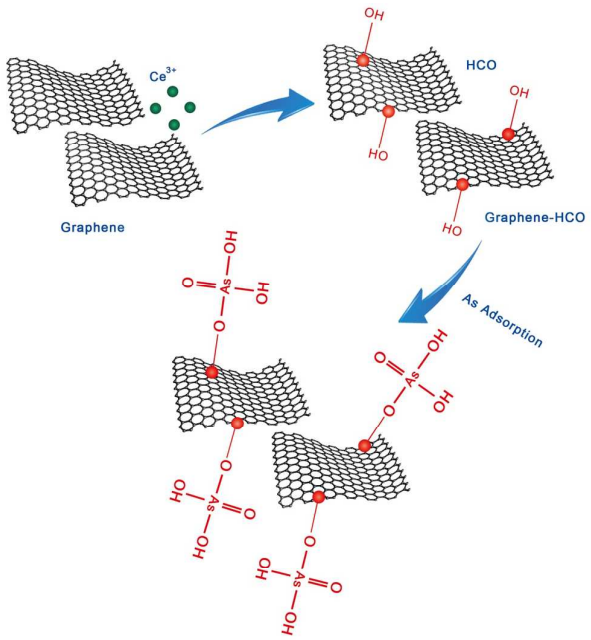

Fig. 9 Schematic diagram of adsorption mechanism of arsenic onto GNP-HCO.

presence of Ce(III). Therefore, the major chemical state of cerium element on the adsorbent is identified as +IV, which may be due to the occurrence of oxidation reaction during the adsorbent preparation.

As shown in Fig. 8, the high resolution scan of O1s spectra of the adsorbents can be divided into metal oxide (M-O), metal-hydroxyl (M-OH) and adsorbed water (H_2O) with the binding energies of 529.68, 531.44 and 532.87 eV (for virgin adsorbent) and 529.77, 531.07 and 532.23eV (for As-loaded adsorbent), respectively.[49-52] After the adsorption, a new component peak with binding energy of 533.57 eV can be attributed to arsenic-oxygen (As-O) bond. After the adsorption, the relative area ratio for the component peak of M-O increases from 32.20% to 46.12%, while the relative area ratios for the peaks due to M-OH and H_2O decrease from 34.33% to 27.75% and 33.47% to 16.72%, respectively. The significant decrease in the area ratio of M-OH group indicates that –OH groups on the surface of the adsorbent may play a certain role for the arsenate adsorption.

The atomic ratios of Ce, O and As in the adsorbents before and after adsorption are listed in Table S2. The atomic faction of the arsenic is increased from 0 % to 2.95% after adsorption process. This indicates that the arsenic can be adsorbed onto the GNP-HCO adsorbent. Meanwhile, the atomic fraction of O decreases remarkably from 77.52 % to 65.40 % after the adsorption. This change further supports the involvement of hydroxyl group in the adsorption process.

Based on the previous results and analysis, the hydroxyl groups of HCO play a significant role in the arsenic removal, and a possible adsorption mechanism of GNP-HCO was proposed, as display in Fig. 9. The M-OH group on the surface of the adsorbent may be protonated at acidic condition which causes an enhanced electrostatic attraction between arsenic and active sites, followed by the occurrence of binding of arsenic on the active sites, and then displaced from the metal binding sites. It is found that the positive charged group is much easier to be substituted than the neutral group which is more favorable to the ligand exchange process.[53] With the increase in solution pH, more hydroxyl groups will be present leading to a stronger competition for the active sites. In parallel, the surface charge of the adsorbent would become more negative and the strong electrostatic repulsion between the active sites and arsenic species would thus hinder the ligands exchange and finally reduce the adsorption capacity.

Conclusions

Hydrous cerium oxide modified graphene was prepared for the removal of arsenic from aqueous solution. The rapid adsorption kinetics and excellent adsorbing capability of GNP-HCO adsorbent provide convincing evidence for its potential use in the treatment of arsenic-contaminated water.

Acknowledgement

The authors acknowledge the financial support from the GE-NUS Research Grant (WBS Number of R-706-005-004-592).

References

1. H. Brammer and P. Ravenscroft, *Environment International*, 2009, **35**, 647-654.
2. M. M. Karim, *Water Research*, 2000, **34**, 304-310.
3. P. Pal, S. Ahammad, A. Pattanayak and P. Bhattacharya, *Water environment research*, 2007, **79**, 357-366.
4. W. H. Ficklin, *Talanta*, 1983, **30**, 371-373.
5. D. Pokhrel, *Removal of Arsenic from Drinking Water by Fungal Biomass and Biological Filtration*, University of Regina (Canada), 2007.

RSC Advances Accepted Manuscript

6. S. M. Miller, M. L. Spaulding and J. B. Zimmerman, *Water Research*, 2011, **45**, 5745-5754.
7. E. Fogarassy, I. Galambos, E. Bekassy-Molnar and G. Vatai, *Desalination*, 2009, **240**, 270-273.
8. K. Sasaki, H. Nakano, W. Wilopo, Y. Miura and T. Hirajima, *Colloids and Surfaces A: Physicochemical and Engineering Aspects*, 2009, **347**, 8-17.
9. N. Horzum, M. M. Demir, M. Nairat and T. Shahwan, *RSC Advances*, 2013, **3**, 7828-7837.
10. M. Asadullah, I. Jahan, M. B. Ahmed, P. Adawiyah, N. H. Malek and M. S. Rahman, *Journal of Industrial and Engineering Chemistry*, 2014, **20**, 887-896.
11. S. Lunge, S. Singh and A. Sinha, *Journal of Magnetism and Magnetic Materials*, 2014, **356**, 21-31.
12. T. Zhang and D. D. Sun, *Chemical Engineering Journal*, 2013, **225**, 271-279.
13. R. Srivastava, *Journal of Colloid and Interface Science*, 2010, **348**, 600-607.
14. G. Jegadeesan, S. R. Al-Abed, V. Sundaram, H. Choi, K. G. Scheckel and D. D. Dionysiou, *Water Research*, 2010, **44**, 965-973.
15. H. Cui, Y. Su, Q. Li, S. Gao and J. K. Shang, *Water Research*, 2013, **47**, 6258-6268.
16. S. Bibi, A. Farooqi, K. Hussain and N. Haider, *Journal of Cleaner Production*, 2015, **87**, 882-896.
17. Suhas, P. J. M. Carrott and M. M. L. Ribeiro Carrott, *Bioresource Technology*, 2007, **98**, 2301-2312.
18. H. S. Park, J. R. Koduru, K. H. Choo and B. Lee, *Journal of Hazardous Materials*, 2015, **286**, 315-324.
19. H. Humbert, H. Gallard, H. Suty and J. P. Croué, *Water Research*, 2008, **42**, 1635-1643.
20. T. Anumol, M. Sgroi, M. Park, P. Roccaro and S. A. Snyder, *Water Research*, 2015, **76**, 76-87.
21. R. K. Joshi, P. Carbone, F. C. Wang, V. G. Kravets, Y. Su, I. V. Grigorieva, H. A. Wu, A. K. Geim and R. R. Nair, *Science*, 2014, **343**, 752-754.
22. K. S. Novoselov, A. K. Geim, S. V. Morozov, D. Jiang, Y. Zhang, S. V. Dubonos, I. V. Grigorieva and A. A. Firsov, *Science*, 2004, **306**, 666-669.
23. J. Zhao, Z. Wang, Q. Zhao and B. Xing, *Environmental Science & Technology*, 2014, **48**, 331-339.
24. Y. Liu, J. H. Dustin Lee, Q. Xia, Y. Ma, Y. Yu, L. Y. Lanry Yung, J. Xie, C. N. Ong, C. D. Vecitis and Z. Zhou, *Journal of Materials Chemistry A*, 2014, **2**, 16554-16562.
25. F. Bonaccorso, L. Colombo, G. Yu, M. Stoller, V. Tozzini, A. C. Ferrari, R. S. Ruoff and V. Pellegrini, *Science*, 2015, **347**.
26. Z. Liu, K. Parvez, R. Li, R. Dong, X. Feng and K. Müllen, *Advanced Materials*, 2015, **27**, 669-675.
27. L. Qiu, Q. Wu, Z. Yang, X. Sun, Y. Zhang and H. Peng, *Small*, 2015, **11**, 1150-1155.
28. S. C. Ray, in *Applications of Graphene and Graphene-Oxide Based Nanomaterials*, ed. S. C. Ray, William Andrew Publishing, Oxford, 2015, pp. 1-38.
29. W. Zhang, J. Fu, G. Zhang and X. Zhang, *Chemical Engineering Journal*, 2014, **251**, 69-79.
30. X. Luo, C. Wang, S. Luo, R. Dong, X. Tu and G. Zeng, *Chemical Engineering Journal*, 2012, **187**, 45-52.
31. V. Chandra, J. Park, Y. Chun, J. W. Lee, I. C. Hwang and K. S. Kim, *ACS Nano*, 2010, **4**, 3979-3986.
32. Y. Zhang, M. Yang and X. Huang, *Chemosphere*, 2003, **51**, 945-952.
33. Y. S. Ho and G. McKay, *Water Research*, 2000, **34**, 735-742.
34. H. Cui, Q. Li, S. Gao and J. K. Shang, *Journal of Industrial and Engineering Chemistry*, 2012, **18**, 1418-1427.
35. X. J. Gong, W. G. Li, D. Y. Zhang, W. B. Fan and X. R. Zhang, *International Biodeterioration & Biodegradation*, 2015, **In press**.
36. C. Shan and M. Tong, *Water Research*, 2013, **47**, 3411-3421.
37. A. Gupta, V. S. Chauhan and N. Sankararamakrishnan, *Water Research*, 2009, **43**, 3862-3870.
38. X. Song, Y. Zhang, C. Yan, W. Jiang and C. Chang, *Journal of Colloid and Interface Science*, 2013, **389**, 213-219.
39. I. Langmuir, *Journal of the American Chemical Society*, 1918, **40**, 1361-1403.
40. A. V. Vitela-Rodriguez and J. R. Rangel-Mendez, *Journal of Environmental Management*, 2013, **114**, 225-231.
41. Z. Sun, Y. Yu, S. Pang and D. Du, *Applied Surface Science*, 2013, **284**, 100-106.
42. A. K. Mishra and S. Ramaprabhu, *The Journal of Physical Chemistry C*, 2010, **114**, 2583-2590.
43. S. P. Dubey, T. T. M. Nguyen, Y.-N. Kwon and C. Lee, *Journal of Industrial and Engineering Chemistry*.
44. G. Sheng, Y. Li, X. Yang, X. Ren, S. Yang, J. Hu and X. Wang, *RSC Advances*, 2012, **2**, 12400-12407.
45. H. Liu, K. Zuo and C. D. Vecitis, *Environmental Science & Technology*, 2014, **48**, 13871-13879.
46. R. Sandoval, A. M. Cooper, K. Aymar, A. Jain and K. Hristovski, *Journal of Hazardous Materials*, 2011, **193**, 296-303.
47. H. Zhu, Y. Jia, X. Wu and H. Wang, *Journal of Hazardous Materials*, 2009, **172**, 1591-1596.
48. E. J. Preisler, O. J. Marsh, R. A. Beach and T. C. McGill, *Journal of Vacuum Science & Technology B*, 2001, **19**, 1611-1618.
49. B. Chen, Z. Zhu, J. Ma, Y. Qiu and J. Chen, *Journal of Materials Chemistry A*, 2013, **1**, 11355-11367.
50. T. Wang, W. Yang, T. Song, C. Li, L. Zhang, H. Wang and L. Chai, *RSC Advances*, 2015, **5**, 50011-50018.
51. Z. Wen, C. Dai, Y. Zhu and Y. Zhang, *RSC Advances*, 2015, **5**, 4058-4068.
52. S. Guo, W. Sun, W. Yang, Q. Li and J. K. Shang, *RSC Advances*, 2015, **5**, 53280-53288.
53. N. I. Chubar, V. A. Kanibolotskyy, V. V. Strelko, G. G. Gallios, V. F. Samanidou, T. O. Shaposhnikova, V. G. Milgrandt and I. Z. Zhuravlev, *Colloids and Surfaces A: Physicochemical and Engineering Aspects*, 2005, **255**, 55-63.

RSC Advances Accepted Manuscript

This journal is © The Royal Society of Chemistry 2015

Please do not adjust margins

Table of contents entry

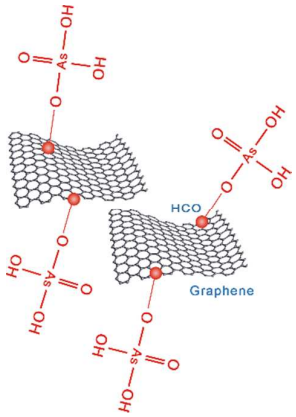

A promising hydrous cerium oxide modified graphene (GNP-HCO) adsorbent with rapid adsorption kinetics and excellent adsorbing capacity towards arsenic removal.

RSC Advances Accepted Manuscript

Please do not adjust margins